Mathematical Biosciences and Engineering

http://www.aimspress.com/journal/mbe

MBE, 21(4): 5881–5899.
DOI: 10.3934/mbe.2024260
Received: 13 February 2024
Revised: 16 April 2024
Accepted: 22 April 2024
Published: 14 May 2024

Research article

Threshold dynamics of a switching diffusion SIR model with logistic growth and healthcare resources

Shuying Wu and Sanling Yuan*

College of Science, University of Shanghai for Science and Technology, Shanghai 200093, China

* **Correspondence:** Email: sanling@usst.edu.cn.

Abstract: In this article, we have constructed a stochastic SIR model with healthcare resources and logistic growth, aiming to explore the effect of random environment and healthcare resources on disease transmission dynamics. We have showed that under mild extra conditions, there exists a critical parameter, i.e., the basic reproduction number R_0^s, which completely determines the dynamics of disease: when $R_0^s < 1$, the disease is eradicated; while when $R_0^s > 1$, the disease is persistent. To validate our theoretical findings, we conducted some numerical simulations using actual parameter values of COVID-19. Both our theoretical and simulation results indicated that (1) the white noise can significantly affect the dynamics of a disease, and importantly, it can shift the stability of the disease-free equilibrium; (2) infectious disease resurgence may be caused by random switching of the environment; and (3) it is vital to maintain adequate healthcare resources to control the spread of disease.

Keywords: stochastic SIR epidemic model; switching diffusion; threshold; backward bifurcation; logistic growth

1. Introduction

Infectious diseases have always been the greatest enemy of mankind, and their proliferation time and again since ancient times has brought great disasters to human life and development. As early as the second century A.D., the Antonine Plague ravaged the Roman Empire, causing a sharp decline in population and economic deterioration, eventually leading to the fall of the Roman Empire [1]. The measles epidemic of 1519–1530 A.D. caused the Mexico Indians to plummet from 30 million to 3 million [2]. The horrific Black Death struck the European continent on three occasions: the first time, in 1346–1350, nearly one-third of Europe's population died during the epidemic; the second time, documented as having occurred in 1665–1666, when one-sixth of London's population died; and the last time, in 1720–1722, killing one-half of the population of Marseilles in France, 60% of the

population of the Toulon neighborhood, 44% of the population of Arles, and 30% of the populations of the Aix and the Arignon [1].

Throughout history, mankind has fought a relentless battle against infectious diseases. Looking back at history, mankind has also won glorious victories in the fight against infectious diseases, and the 20th century can be said to be the most glorious period in which mankind conquered infectious diseases. Examples include defeating smallpox, which had ravaged the world for more than 2000 years [3]; leprosy and polio are about to be eradicated [4,5]; and diphtheria, measles, tetanus, and other infectious diseases have also been effectively controlled [6–8]. But the road to conquering infectious diseases is still long and winding. According to the World Health Organization (WHO), infectious diseases remain the number one killer of humans. For instance, as of 2021, about 38.4 million people worldwide live with HIV, with about 1.5 million new infections and about 650,000 deaths in 2021 [9]; as well as more than 772 million confirmed cases of COVID-19 and more than 6.9 million deaths worldwide as of January 2024 [10]. History and reality tell us that mankind is facing a strong challenge of infectious diseases, and the study of the transmission mechanism, transmission rules, and prevention and control strategies of a certain infectious disease have become major problems that need to be urgently solved in today's world.

It is well known that establishing mathematical models is an important theoretical approach to studying the transmission mechanisms and transmission dynamics of infectious diseases. For example, as early as 1760, Bernouli had studied the spread of smallpox using mathematical methods [4]. In 1906, Hamer constructed a discrete model to study the recurrent epidemiologic process of measles [11]. In 1911, Ross [12] used a differential equation model to study the dynamic behavior of malaria transmission between mosquitoes and humans, and showed that if mosquito populations are kept below a threshold, malaria transmission can be effectively controlled, for which Ross received the Nobel Prize in Medicine. In 1927, Kemack and McKendrick [13] investigated the transmission patterns of the Black Death epidemic in London in 1665–1666 and of the plague in Bombay in 1906 by constructing the classical SIR compartmentalization model, and then in 1932, they proposed the "Threshold Theory" for determining whether or not an infectious disease would eventually become an epidemic [14], which laid a solid theoretical foundation for subsequent research on the dynamics of infectious diseases. Over the past 40 years, many scholars have conducted in-depth and systematic studies on infectious disease dynamics based on their predecessors and have achieved fruitful results. A large number of epidemic models are proposed to study the transmission patterns of various epidemics, especially for measles, malaria, tuberculosis, AIDS/HIV, SARS, dengue fever, influenza, and COVID-19 [15–18].

Classical epidemic models usually assume a constant size of the total population or a constant rate of recruitment of the susceptible class [19–23]. This indicates that population size changes exponentially, except for equal birth and death rates. This pattern of growth is unrealistic, as it only occurs when there are sufficient resources [24–26], since nutrients and suitable environments are becoming more limited as population size increases [27]. In this sense, logistic growth seems to be more realistic. To this end, a variety of epidemic models with logistic growth have been proposed by many leading scholars, such as Liu et al. [25] who constructed two avian influenza bird-to-human transmission models with logistic growth, and analyzed their dynamical behavior.

During an outbreak, there are frequently no effective treatments or vaccines available, and the limited scope for preventing or controlling the spread of the outbreak will result in a sudden increase in the demand for emergency supplies and medical resources, leading to a temporary shortage of

supplies. For example, during the outbreak of COVID-19 in Wuhan, thousands of volunteer doctors from all over China supported Wuhan, and aid supplies from all provinces of China were transported to Wuhan in a race against time. To accommodate the large number of confirmed cases, the Vulcan Mountain and Thunder Mountain hospitals were established [28, 29]. In classical epidemic models, the recovery rate is usually proportional to the number of infected individuals [23, 24]. This recovery rate has limitations since it requires unlimited medical resources. Therefore, it is particularly important to consider the impact of healthcare resources on the dynamics of outbreak transmission when modeling epidemics. To reveal the impact of healthcare resources on epidemic transmission dynamics, Shan and Zhu [19] assumed that the recovery rate depended on the abundance of healthcare resources and the number of infected individuals, and more precisely, it was positively correlated with healthcare resources and negatively correlated with the number of infected individuals. According to the WHO Statistical Information System, the number of available hospital beds per 10,000 population is an important indicator of the abundance of healthcare resources [19]. Hence, Shan and Zhu [19] proposed the following recovery rate with the number of hospital beds:

$$\mu = \mu(b, I) = \mu_0 + \frac{(\mu_1 - \mu_0)b}{I + b}, \tag{1.1}$$

where μ_0 and μ_1 are the minimum and maximum recovery rates, respectively. Parameter b is the number of hospital beds. I is the infective class. Their study shows that variations in the number of hospital beds can lead to complex dynamical behaviors of disease transmission and that maintaining an adequate number of beds is essential for controlling infectious diseases. The recovery rate equation (1.1) was applied by Abdelrazec et al. [19] to study the impact of resources available to the health system on dengue transmission dynamics. In addition, Saha and Ghosh [26] considered the impact of limited environmental resources on population size and the number of hospital beds on the recovery rate and constructed the following SIR model:

$$\begin{cases} \frac{\mathrm{d}S}{\mathrm{d}t} = rS\left(1 - \frac{S}{K}\right) - \frac{\beta S I}{1+\alpha I^2} - u_1 S, \\ \frac{\mathrm{d}I}{\mathrm{d}t} = \frac{\beta S I}{1+\alpha I^2} - (d+\delta)I - \left(\mu_0 + \frac{(\mu_1-\mu_0)b}{b+I}\right) I, \\ \frac{\mathrm{d}R}{\mathrm{d}t} = \left(\mu_0 + \frac{(\mu_1-\mu_0)b}{b+I}\right) I + u_1 S - dR, \end{cases} \tag{1.2}$$

where S and R represent, respectively, the susceptible and recovered classes. r denotes the intrinsic growth rate of susceptible individuals. β is the disease transmission rate, α measures the psychological effect, u_1 is the rate of newborn susceptible population vaccinated, d and δ denote natural mortality and disease-related mortality, respectively. Notice that the third equation of model (1.2) does not affect its first two equations, and we thus consider only its sub-model as follows

$$\begin{cases} \frac{\mathrm{d}S}{\mathrm{d}t} = rS\left(1 - \frac{S}{K}\right) - \frac{\beta S I}{1+\alpha I^2} - u_1 S, \\ \frac{\mathrm{d}I}{\mathrm{d}t} = \frac{\beta S I}{1+\alpha I^2} - (d+\delta)I - \left(\mu_0 + \frac{(\mu_1-\mu_0)b}{b+I}\right) I. \end{cases} \tag{1.3}$$

Many studies have shown that climatic factors have a significant impact on the dynamics of disease transmission. For example, Robert's study showed that the activity of respiratory syncytial virus reached its maximum at 45–65% relative humidity [30]. The rate of transmission of COVID-19 is nonlinearly correlated with its ambient temperature [31]; low temperature favors the survival and multiplication of SARS-CoV-2 in the environment, and low humidity makes the virus less likely to

settle, which facilitates the spread of the virus through the air [32]. Thus, stochastic environments have a significant impact on the transmission dynamics of epidemics and cannot be neglected.

One approach is to employ stochastic differential equations driven by Gaussian white noise to examine how environmental fluctuations affect the persistence or elimination of infectious illnesses [20, 33, 34]. Examining models of stochastic differential equations driven by Markov chains, also known as systems with telegraph noise, is another viable strategy [35–37]. The difficulty with foreseeing the pathogens transition across environments, as various environmental conditions will result in varying levels of pathogen survival and infectivity, is a fundamental intuitive justification for the adoption of systems with telegraph noise [38]. A system with telegraph noise uses sets of ordinary differential equations to model the transmission dynamics of epidemics at different time periods. Once the environment changes, the pattern of disease transmission changes, which in turn causes the ordinary differential equations describing the pattern of disease transmission to change. The process is then repeated indefinitely [38]. In this paper, we suppose that the disease transmission rate β is perturbed by white noise and Markov switching, and establish the following stochastic model:

$$\begin{cases} \mathrm{d}S(t) = \left(rS\left(1-\frac{S}{K}\right) - \frac{\beta(\upsilon(t))SI}{1+\alpha I^2} - u_1 S\right)\mathrm{d}t - \frac{\sigma SI}{1+\alpha I^2}\mathrm{d}B(t), \\ \mathrm{d}I(t) = \left(\frac{\beta(\upsilon(t))SI}{1+\alpha I^2} - (d+\delta)I - \left(\mu_0 + \frac{(\mu_1-\mu_0)b}{b+I}\right)I\right)\mathrm{d}t + \frac{\sigma SI}{1+\alpha I^2}\mathrm{d}B(t), \end{cases} \tag{1.4}$$

where σ represents the white noise intensity, $B(t)$ denotes the Brownian motion, $\upsilon(t)$ is a right continuous Markov chain in a finite state space $\mathcal{H} = \{1, 2, \cdots, \mathcal{N}\}$ with the generator $\mathcal{W} = (\mathfrak{f}_{ij})_{\mathcal{N}\times\mathcal{N}}$ given by

$$\mathbb{P}\{\upsilon(t+\Delta t) = j | \upsilon(t) = i\} = \begin{cases} \mathfrak{f}_{ij}\Delta t + o(\Delta t) & \text{if } i \neq j, \\ 1 - \sum\limits_{i\neq k} \mathfrak{f}_{ik}\Delta t + o(\Delta t) \text{ if } i = j, \end{cases} \tag{1.5}$$

where $\Delta t > 0$ and $\mathfrak{f}_{ij} \geq 0$ is the transition rate from regime i to regime j ($i \neq j$).

Compared to the results of stochastic epidemic models with healthcare resources, e.g., [20, 33, 35], this paper has the following advantages:

- Threshold dynamics of a switching diffusion SIR model with logistic growth and healthcare resources are investigated.
- If $\sigma = 0$, and the elements of the generator $\mathcal{W}$ are increased to a certain value, then the solution of stochastic model (1.4) almost coincides with the solution of deterministic model (1.3) with $\beta = \sum_{i\in\mathcal{H}} \pi_i \beta(i)$.

In this sense, we extend the previous studies.

The remainder of the paper is organized as follows: Section 2 examines the disease persistence and extinction for stochastic model (1.4). In Section 3, we use the actual parameter values to simulate and validate our theoretical results and give some biological explanations. Finally, the conclusions of the paper are presented and discussed in Section 4.

2. Dynamical behavior for stochastic model (1.4)

Throughout, we assume that the Brownian motion $B(t)$ is defined on a complete probability space $(\Omega, \mathcal{F}, \{\mathcal{F}_t\}_{t\geq 0}, \mathbb{P})$ and that υ is independent of $B(t)$. Let

$$\mathbb{R}^k_+ = \{y \in \mathbb{R}^k | y_i > 0, i = 1, 2, \cdots, k\}.$$

Suppose that the Markov chain $\upsilon(t)$ is irreducible, then there is a unique stationary distribution $\pi = (\pi_1, \ldots, \pi_{\mathcal{N}}) \in \mathbb{R}_+^{\mathcal{N}}$ with

$$\pi \mathcal{W} = 0, \text{ and } \sum_{s=1}^{\mathcal{N}} \pi_s = 1.$$

For the theories and notations related to stochastic differential equations with regime switching, the reader is referred to [35, 38, 39].

Before delving into our examination of the fundamental characteristics of stochastic model (1.4), we first provide the positivity of the solution for the model. The proof is routine and is, therefore, left out.

Theorem 2.1. *Model* (1.4) *has a unique global positive solution with probability 1 for any initial condition* $(S(0), I(0)) \in \mathbb{R}_+^2$. *Furthermore, there exists* $\tau > 0$ *such that*

$$0 < S(t) + I(t) < \frac{K(r + d - u_1)^2}{4rd}, \ \forall t \geq \tau.$$

Notice that $(0, 0)$ is an equilibrium of model (1.4), so we need to investigate under what conditions the equilibrium $(0, 0)$ is unstable. If $(0, 0)$ is stable, then the system is collapsing.

Theorem 2.2. *If* $r > u_1$, *then for any initial value* $(S(0), I(0)) \in \mathbb{R}_+^2$, *there exists a constant* $\tilde{c} := \tilde{c}(S(0), I(0)) > 0$ *such that*

$$\mathbb{P}\left\{\inf_{t \geq 0} S(t) \geq \tilde{c}\right\} = 1. \tag{2.1}$$

Proof. Define $V_1 = S^{-\theta_1}$, where $\theta_1 > 0$. By Itô's formula [40], we have

$$LV_1 = -\theta_1 S^{-\theta_1}\left(r - u_1 - \frac{rS}{K} - \frac{\beta(\upsilon(t))I}{1 + \alpha I^2} - \frac{\sigma^2 I^2}{2(1 + \alpha I^2)^2}\right). \tag{2.2}$$

Assume that D_ϵ is a deleted neighborhood of $(0, 0)$, and $\epsilon > 0$ is a small enough constant. Then it follows from Eq (2.2) that for any $(S, I) \in D_\epsilon$,

$$LV_1 \leq -\theta_1 S^{-\theta_1}\left(r - u_1 - f(\epsilon)\right),$$

where $f(\epsilon)$ is a function that is continuous at 0 and $f(0) = 0$. Hence, for sufficiently small ϵ and any $(S, I) \in D_\epsilon$, we have

$$LV_1 \leq -\theta_1 S^{-\theta_1}\left(r - u_1 - f(\epsilon)\right) < 0.$$

On the basis of Lemma 7.7 in [38], we know that $(0, 0)$ is unstable in probability. □

Based on Theorems 2.1 and 2.2, we easily obtain that if $r > u_1$, the feasible domain Γ is almost surely positively invariant, where

$$\Gamma = \left\{(S, I) \in \mathbb{R}_+^2 : 0 < S + I < \frac{K(r + d - u_1)^2}{4rd}, S \geq \tilde{c}\right\}. \tag{2.3}$$

As such, we solely examine the dynamics of model (1.4) in Γ, when $r > u_1$.

Determining the threshold condition for disease extinction and persistence is an important topic in the study of epidemic dynamics. First, we introduce one of the most central indicators in epidemiology for model (1.4), i.e., the basic reproduction number:

$$R_0^s := \frac{K(r-u_1)}{r\left(d+\delta+\mu_1+\frac{\sigma^2K^2(r-u_1)^2}{2r^2}\right)}\cdot\sum_{k\in\mathcal{H}}\pi_k\beta(k), \tag{2.4}$$

which is often used to characterize the rate of transmission of the epidemic, reflecting the potential and severity of the outbreak. Next, we will demonstrate that R_0^s is the threshold value that establishes whether the illness is extinct or not.

Theorem 2.3. *If $r > u_1$ and $R_0^s < 1$, then the disease-free equilibrium $\left(\frac{K(r-u_1)}{r}, 0\right)$ for stochastic model* (1.4) *is almost surely globally asymptotically stable.*

Proof. The theorem's proof is broken down into three steps as follows.

Step 1. We demonstrate the local asymptotic stability of the disease-free equilibrium $\left(\frac{K(r-u_1)}{r}, 0\right)$, that is, there exists a constant $\varrho_1 > 0$ such that

$$\mathbb{P}\left\{\lim_{t\to\infty}(S(t), I(t)) = \left(\frac{K(r-u_1)}{r}, 0\right)\right\} \geq 1-\varepsilon \tag{2.5}$$

for any $\varepsilon > 0$ and any $(S(0), I(0)) \in O_{\varrho_1} := \left(\frac{K(r-u_1)}{r} - \varrho_1, \frac{K(r-u_1)}{r} + \varrho_1\right) \times (0, \varrho_1)$.

In fact, using Itô's formula yields

$$\mathrm{d}\ln I = L\ln I\mathrm{d}t + \frac{\sigma S}{1+\alpha I^2}\mathrm{d}B(t) \tag{2.6}$$

where

$$\begin{aligned} L\ln I =& \frac{\beta(\upsilon(t))S}{1+\alpha I^2} - (d+\delta) - \left(\mu_0 + \frac{(\mu_1-\mu_0)b}{b+I}\right) - \frac{\sigma^2S^2}{2(1+\alpha I^2)^2} \\ =& \left(\frac{\beta(\upsilon(t))K(r-u_1)}{r} - (d+\delta+\mu_1) - \frac{\sigma^2K^2(r-u_1)^2}{2r^2}\right) \\ &+ \left(\frac{\beta(\upsilon(t))S}{1+\alpha I^2} - \frac{\beta(\upsilon(t))K(r-u_1)}{r}\right) - \left(\mu_0 + \frac{(\mu_1-\mu_0)b}{b+I} - \mu_1\right) \\ &- \frac{\sigma^2}{2}\left(\frac{S^2}{(1+\alpha I^2)^2} - \frac{K^2(r-u_1)^2}{r^2}\right) \\ :=& f_1(S, I, \upsilon(t)). \end{aligned} \tag{2.7}$$

Note that

$$\lim_{\substack{I\to 0\\ S\to K(r-u_1)/r}} f_1(S, I, \upsilon(t)) = \left(\frac{\beta(\upsilon(t))K(r-u_1)}{r} - (d+\delta+\mu_1) - \frac{\sigma^2K^2(r-u_1)^2}{2r^2}\right),$$

and $f_1(S, I, \upsilon(t))$ is a continuous function concerning $(S, I) \in \Gamma$. Hence, for any $\epsilon > 0$ and all $(S, I) \in O_{\varrho_1}$, there is a sufficiently small $\varrho_1 > 0$ such that

$$f_1(S, I, \upsilon(t)) < \left(\frac{\beta(\upsilon(t))K(r-u_1)}{r} - (d+\delta+\mu_1) - \frac{\sigma^2K^2(r-u_1)^2}{2r^2}\right) + \epsilon. \tag{2.8}$$

By combining Eqs (2.6) and (2.8), the strong law of large numbers and the Birkhoff ergodic theorem together, we can demonstrate that

$$\limsup_{t\to\infty}\frac{\ln I(t)}{t}\le\left(\frac{K(r-u_1)}{r}\sum_{k\in\mathcal{H}}\pi_k\beta(k)-(d+\delta+\mu_1)-\frac{\sigma^2K^2(r-u_1)^2}{2r^2}\right)+\epsilon.$$

Since ϵ is arbitrarily small and $R_0^s<1$, we have

$$\limsup_{t\to\infty}\frac{\ln I(t)}{t}<0,$$

i.e.,

$$\lim_{t\to\infty}I(t)=0\ a.s.$$

Then we easily get

$$\lim_{t\to\infty}S(t)=\frac{K(r-u_1)}{r}\ a.s.$$

Therefore, Equation (2.5) holds.

Step 2. We show that for any $(S(0),I(0))\in\Gamma$, the solution of stochastic model (1.4) always arrives at

$$D_{\varrho_1}:=\left\{(S,I):\ S\in\left(\frac{K(r-u_1)}{r}-\frac{\sqrt{2}\varrho_1}{2},\frac{K(r-u_1)}{r}+\frac{\sqrt{2}\varrho_1}{2}\right)\text{ and }I\in\left(0,\frac{\sqrt{2}\varrho_1}{2}\right)\right\}$$

which is a subset of O_{ϱ_1} at some moment whenever $R_0^s<1$. We can assume $(S(0),I(0))\in\Gamma\setminus D_{\varrho_1}$, and then the first hitting time of set D_{ϱ_1} is defined by $\tau_{\varrho_1}:=\inf\{t\ge0,(S(t),I(t))\in D_{\varrho_1}\}$. It then follows from Theorem 2.2 that there exists $S_{\min}>0$ such that $S(t)\ge S_{\min}$ for any $t\in[0,\tau_{\varrho_1}]$. Hence, there is a sufficiently large constant ℓ_2 such that

$$\frac{\sqrt{2}r\varrho_1S_{\min}}{2K}-\beta(\upsilon(t))\left(\frac{K(r+d-u_1)^2}{4rd}+1\right)\frac{SI}{1+\alpha I^2}+\frac{(\ell_2-1)\sigma^2}{2}\left(\frac{SI}{1+\alpha I^2}\right)^2<0$$

for all $(S,I)\in\Gamma\setminus D_{\varrho_1}$. Then, define sufficiently large positive constant ℓ_1 such that $\Upsilon=\ell_1-(S+1)^{\ell_2}>0$ for $(S,I)\in\Gamma$. According to Itô's formula, we can obtain that

$$\begin{aligned}
L\Upsilon=&-\ell_2(S+1)^{\ell_2-2}\left((S+1)\left[\frac{rS}{K}\left(\frac{K(r-u_1)}{r}-S\right)-\frac{\beta(\upsilon(t))SI}{1+\alpha I^2}+\right]+\frac{(\ell_2-1)\sigma^2S^2I^2}{2(1+\alpha I^2)^2}\right)\\
\le&-\ell_2(S+1)^{\ell_2-2}\left((S+1)\left[\frac{\sqrt{2}r\varrho_1S_{\min}}{2K}-\frac{\beta(\upsilon(t))SI}{1+\alpha I^2}\right]+\frac{(\ell_2-1)\sigma^2S^2I^2}{2(1+\alpha I^2)^2}\right)\\
\le&-\ell_2(S+1)^{\ell_2-2}\left(\frac{\sqrt{2}r\varrho_1S_{\min}}{2K}-\beta(\upsilon(t))\left(\frac{K(r+d-u_1)^2}{4rd}+1\right)\frac{SI}{1+\alpha I^2}+\frac{(\ell_2-1)\sigma^2}{2}\left(\frac{SI}{1+\alpha I^2}\right)^2\right)\\
\le&-\ell_2(S+1)^{\ell_2-2}\left(\frac{\sqrt{2}r\varrho_1S_{\min}}{2K}-\frac{\beta(\upsilon(t))^2\left(\frac{K(r+d-u_1)^2}{4rd}+1\right)^2}{2(\ell_2-1)\sigma^2}\right)\\
\le&-\ell_2(S+1)^{\ell_2-2}\left(\frac{\sqrt{2}r\varrho_1S_{\min}}{4K}\right)\\
\le&-\varrho_1.
\end{aligned}$$

It is easily obtainable from Dynkin's formula that

$$\mathbb{E}[\Upsilon(S(\tau_{\varrho_1} \wedge t), I(\tau_{\varrho_1} \wedge t))] \leq \Upsilon(0) - \frac{1}{2}\varrho_1 \mathbb{E}(\tau_{\varrho_1} \wedge t).$$

Thus by the Fatou's lemma, one has

$$\mathbb{E}[\Upsilon(S(\tau_{\varrho_1}), I(\tau_{\varrho_1}))] \leq \Upsilon(0) - \frac{1}{2}\varrho_1 \mathbb{E}(\tau_{\varrho_1}).$$

Notice that $\Upsilon > 0$, which implies that $\mathbb{E}(\tau_{\varrho_1}) < \infty$.

Step 3. Based on Steps 1 and 2, and the strong Markov property, we easily get that for any $\varepsilon > 0$ and any $(S(0), I(0)) \in \Gamma$,

$$\mathbb{P}\left\{\lim_{t\to\infty}(S(t), I(t)) = \left(\frac{K(r-u_1)}{r}, 0\right)\right\} \geq 1 - \varepsilon.$$

By the arbitrariness of ε, one can see that for each $(S(0), I(0)) \in \Gamma$,

$$\mathbb{P}\left\{\lim_{t\to\infty}(S(t), I(t)) = \left(\frac{K(r-u_1)}{r}, 0\right)\right\} = 1.$$

This accomplishes the proof of the theorem. □

Next, we examine the persistence of the disease, which is a favorite topic in epidemiologic research. We begin with the following conclusion.

Lemma 2.4. *If $r > u_1$ and $R_0^s > 1$, then for any $(S(0), I(0)) \in \{(S, I) \in \Gamma : I = 0\}$, there is $T > 0$ such that*

$$\mathbb{E}\int_0^T f_1(S(t), I(t), \upsilon(t))dt \geq \frac{3\lambda}{4}T, \tag{2.9}$$

where $f_1(S(t), I(t), \upsilon(t))$ is defined in Eq (2.7) and $\lambda = \lim_{t\to\infty} \frac{1}{t}\int_0^t f_1\left(\frac{K(r-u_1)}{r}, 0, \upsilon(s)\right)ds$.

Proof. Notice that $I = 0$ is the solution to the second equation of model (1.4), therefore, when $I(0) = 0$, model (1.4) becomes

$$\begin{cases} \frac{\mathrm{d}S}{\mathrm{d}t} = rS\left(1 - \frac{S}{K}\right) - u_1 S, \\ \frac{\mathrm{d}I}{\mathrm{d}t} = 0. \end{cases}$$

Hence, for each $(S(0), I(0)) \in \{(S, I) \in \Gamma : I = 0\}$, we have

$$\lim_{t\to\infty}(S(t), I(t)) = \left(\frac{K(r-u_1)}{r}, 0\right).$$

That is

$$\lim_{t\to\infty}\frac{1}{t}\int_0^t f_1(S(s), I(s), \upsilon(s))\mathrm{d}s = \lim_{t\to\infty}\frac{1}{t}\int_0^t f_1\left(\frac{K(r-u_1)}{r}, 0, \upsilon(s)\right)\mathrm{d}s = \lambda.$$

It then follows from $R_0^s > 1$ that $\lambda > 0$. Hence, there exists a constant $T > 0$ such that Eq (2.9) holds. □

Theorem 2.5. *If $r > u_1$ and $R_0^s > 1$, there is a constant $\varsigma := \varsigma(S(0), I(0)) > 0$ such that*

$$\liminf_{t\to\infty} \mathbb{P}\{I(t) > \varsigma\} = 1. \tag{2.10}$$

Proof. Define $V_\vartheta = I^\vartheta$, where $\vartheta \in \mathbb{R}$. It follows from Itô's formula that

$$LV_\vartheta = \vartheta\left[\frac{\beta(\upsilon(t))S}{1+\alpha I^2} - (d+\delta) - \left(\mu_0 + \frac{(\mu_1-\mu_0)b}{b+I}\right) + \frac{(\vartheta-1)\sigma^2 S^2}{2(1+\alpha I^2)^2}\right] I^\vartheta. \tag{2.11}$$

Denoting

$$\Lambda_\vartheta = \sup_{(S,I)\in\Gamma}\left\{\vartheta\left[\frac{\beta(\upsilon(t))S}{1+\alpha I^2} - (d+\delta) - \left(\mu_0 + \frac{(\mu_1-\mu_0)b}{b+I}\right) + \frac{(\vartheta-1)\sigma^2 S^2}{2(1+\alpha I^2)^2}\right]\right\},$$

that is, for all $(S(0), I(0)) \in \Gamma$, we have $LV_\vartheta \le \Lambda_\vartheta I^\vartheta$. Hence

$$\mathbb{E}(I^\vartheta(t)) = \mathbb{E}(I^\vartheta(0)) + \mathbb{E}\int_0^t LV_\vartheta \mathrm{d}s \le \mathbb{E}(I^\vartheta(0)) + \int_0^t \Lambda_\vartheta \mathbb{E}(I^\vartheta(s))\mathrm{d}s.$$

It then follows from Gronwall inequality that for any $(S(0), I(0)) \in \Gamma$,

$$\mathbb{E}(I^\vartheta(t)) \le I^\vartheta(0)\exp(\Lambda_\vartheta t), \forall t \ge 0. \tag{2.12}$$

Analogously, for any $t \ge jT$, we have

$$\mathbb{E}(I^\vartheta(t)) \le \mathbb{E}(I^\vartheta(jT))\exp[\Lambda_\vartheta(t-jT)]. \tag{2.13}$$

Define $W(t) = \ln I(0) - \ln I(t)$. Based on Eq (2.7),

$$W(t) = -\int_0^t f_1(S(u), I(u), \upsilon(u))\mathrm{d}u - \int_0^t \frac{\sigma S(u)}{1+\alpha I^2(u)}\mathrm{d}B(u). \tag{2.14}$$

Combining Eq (2.14), the Feller property, and Lemma 2.4, there exists a sufficiently small $\varrho_3 > 0$ such that for each $(S(0), I(0)) \in \{(S, I) \in \Gamma : I < \varrho_3\}$,

$$\mathbb{E}(W(T)) = -\mathbb{E}\int_0^T f_1(S(u), I(u), \upsilon(u))\mathrm{d}u \le -\frac{\lambda}{2}T. \tag{2.15}$$

Hence, for any $t \ge 0$, according to Eq (2.12), we have

$$\mathbb{E}(e^{W(t)} + e^{-W(t)}) = \mathbb{E}\Big(\frac{I(0)}{I(t)} + \frac{I(t)}{I(0)}\Big) \le \quad \mathbb{E}(e^{\Lambda_{-1}t} + e^{\Lambda_1 t}) < \infty. \tag{2.16}$$

Using Lemma 2.2 in [36], we obtain

$$\ln \mathbb{E}(e^{\vartheta W(T)}) \le \mathbb{E}(\vartheta W(T)) + \hat{\Lambda}_1\vartheta^2, \ \vartheta \in [0, 0.5],$$

where $\hat{\Lambda}_1 := \hat{\Lambda}_1(T, \Lambda_{-1}, \Lambda_1)$ is a constant. We then choose sufficiently small ϑ such that $\hat{\Lambda}_1\vartheta^2 \le \frac{\lambda\vartheta}{4}T$. On the basis of Eq (2.15), one can get that

$$\mathbb{E}\Big(\frac{I^\vartheta(0)}{I^\vartheta(T)}\Big) = \mathbb{E}(e^{\vartheta W(T)}) \le \exp\Big(-\frac{\lambda\vartheta}{2}T + \hat{\Lambda}_1\vartheta^2\Big) \le \exp\Big(-\frac{\lambda\vartheta}{4}T\Big).$$

That is, for any $I(0) < \varrho_3$, we have

$$\mathbb{E}(I^{-\vartheta}(T)) \leq I^{-\vartheta}(0)\exp\Big(-\frac{\lambda\vartheta}{4}T\Big) = \rho I^{-\vartheta}(0), \tag{2.17}$$

where $\rho = \exp(-\frac{\lambda\vartheta}{4}T)$.

For any $I(0) > \varrho_3$, it then follows from Eq (2.12) that

$$\mathbb{E}(I^{-\vartheta}(T)) \leq \varrho_3^{-\vartheta}\exp(\Lambda_{-\vartheta}T) := \kappa. \tag{2.18}$$

Combining Eqs (2.18) and (2.17), we easily get that

$$\mathbb{E}(I^{-\vartheta}(T)) \leq \rho I^{-\vartheta}(0) + \kappa,$$

for each $(S(0), I(0)) \in \Gamma$. Based on the Markov property, we immediately get that

$$\mathbb{E}[I^{-\vartheta}((j+1)T)] \leq \rho\mathbb{E}(I^{-\vartheta}(jT)) + \kappa.$$

Therefore

$$\mathbb{E}[I^{-\vartheta}((j+2)T)] \leq \rho^2\mathbb{E}(I^{-\vartheta}(jT)) + \rho\kappa + \kappa,$$

and

$$\mathbb{E}(I^{-\vartheta}(mT)) \leq \rho^m I^{-\vartheta}(0) + \frac{\kappa(1-\rho^m)}{1-\rho}. \tag{2.19}$$

Combining Eqs (2.13) and (2.19) yields

$$\mathbb{E}(I^{-\vartheta}(t)) \leq \Big(\rho^m I^{-\vartheta}(0) + \frac{\kappa(1-\rho^m)}{1-\rho}\Big)\exp(\Lambda_{-\vartheta}T),\ t \in [mT, (m+1)T],$$

which implies that

$$\limsup_{t\to\infty}\mathbb{E}(I^{-\vartheta}(t)) \leq \frac{\kappa}{1-\rho}\exp(\Lambda_{-\vartheta}T) := \Phi.$$

Then, in accordance with Chebyshev's inequality, we easily get

$$\mathbb{P}\{|I(t)| < \iota\} = \mathbb{P}\left\{\frac{1}{|I(t)|^{\vartheta}} > \frac{1}{\iota^{\vartheta}}\right\} \leq \iota^{\vartheta}\mathbb{E}(|I^{-\vartheta}(t)|),$$

where $\iota = \frac{\varepsilon^{\frac{1}{\vartheta}}}{\Phi^{\frac{1}{\vartheta}}}$ and $\varepsilon > 0$ is an arbitrarily small constant. Hence

$$\limsup_{t\to\infty}\mathbb{P}\{|I(t)| < \iota\} \leq \iota^{\vartheta}\Phi = \varepsilon.$$

That is

$$\liminf_{t\to\infty}\mathbb{P}\{I(t) \geq \iota\} > 1 - \varepsilon.$$

The proof of the theorem is hereby finished.

□

3. Numerical results

In this section, we verify and extend our mathematical results by borrowing the actual parameter values from Tamil Nadu for COVID-19. For the sake of convenience, let us first assume that the total resident population of a district in Tamil Nadu is 10,000. As reported in [41], in Tamil Nadu, there are 1.1 hospital beds for every 1000 people. Thus, an estimate of b is 11. In this section, if the value of the numerical solution $I(t)$ at a moment t is less than 0.0001, the illness is deemed extinct. Table 1 summarizes the parameter values for models (1.3) and (1.4).

Table 1. Parameter values for model (1.3) in numerical simulations.

Parameters	Value	Sources
r	0.0077	[42]
K	10,000	Estimated
α	0.0001	Estimated
u_1	0.0027	Estimated
d	0.0061	[43]
δ	0.0122	[44]
μ_0	1/34	[45]
μ_1	1/16	[45]
b	11	[41]
$R_0 := \frac{\beta K(r-u_1)}{r(d+\delta+\mu_1)}$	1.405	[46]

We always assume that $S(0) = 6200$, $I(0) = 10$, and $R(0) = 3790$, unless otherwise stated. As shown in [47] and [48], SARS-CoV-2 is highly stable in cold environments at 4°C, whereas after the temperature reaches 20°C, SARS-CoV-2 survival decreases with the increasing temperature. Hence, based on Table 1, we assume that the basic reproduction numbers in states 1 (cold environments) and 2 (hot environments) are respectively

$$R_0(1) := \frac{\beta(1)K(r-u_1)}{r\left(d+\delta+\mu_1+\frac{\sigma^2K^2(r-u_1)^2}{2r^2}\right)} = 1.405, R_0(2) := \frac{\beta(2)K(r-u_1)}{r\left(d+\delta+\mu_1+\frac{\sigma^2K^2(r-u_1)^2}{2r^2}\right)} = 0.797,$$

and we can get the transmission rates in states 1 and 2, respectively, as $\beta(1) = 1.7623 \times 10^{-5}$, $\beta(2) = 1.0 \times 10^{-5}$.

It is well known that white noise can inhibit disease outbreaks when its intensity is sufficiently high. Therefore, this issue will not be addressed in this paper. Backward bifurcation is a problem of coexistence of multiple equilibria for the model, which is a hot research topic in the epidemic model. A discussion similar to Theorem 10 in [26], one can get that deterministic model (1.3) undergoes backward bifurcation at $R_0 = 1$ if $b < \frac{K(\mu_1-\mu_0)(r-u_1)^2}{r(d+\delta+\mu_1)}$. Hence, in this section, we focus on how white noise and random switching affect the dynamics of the transmission dynamics for the disease when deterministic model (1.3) undergoes backward bifurcation. To do this, we let β vary and fix the other parameters such that R_0 varies between 0.75 and 1.1, and $b = 11 < \frac{K(\mu_1-\mu_0)(r-u_1)^2}{r(d+\delta+\mu_1)} = 13.085275$. As shown in Figure 1, deterministic model (1.3) has two endemic equilibrium and one disease-free

equilibrium when $0.7961 < R_0 < 1$, and both the disease-free equilibrium and endemic equilibrium with a relatively large number of infected individuals are stable. We then divide the numerical simulation into three parts as follows.

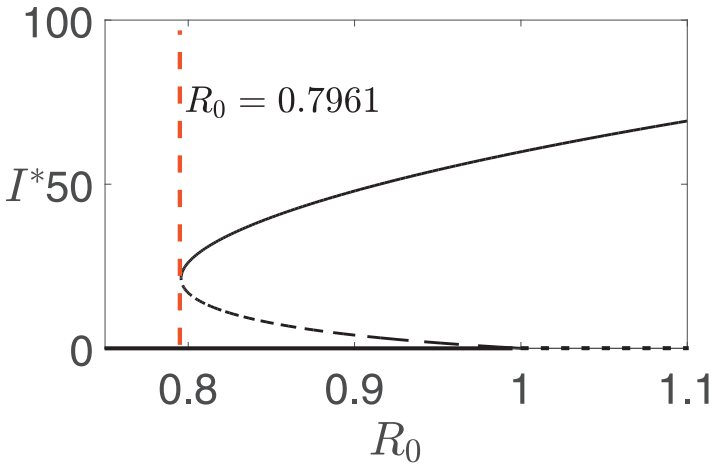

Figure 1. The backward bifurcation curve for model (1.3).

3.1. Impact of white noise on the transmission dynamics for the disease

We first let $\mathcal{N} = 1, \beta(\upsilon(t)) \equiv 1.15246\times10^{-5}, \sigma = 0.000001$, and the other parameters are taken from Table 1. A direct calculation gives $R_0 = 0.9188$ and $R_0^s = 0.9186$. As shown in Figure 2, deterministic model (1.3) with $\beta \equiv 1.15246 \times 10^{-5}$ has two endemic equilibrium E_1 and E_2, and the disease-free equilibrium E_0. Moreover, both E_2 and E_0 are stable, while E_1 is a saddle point. Further, the stable manifold of E_1 divides $\mathbb{R}^2_+$ into two regions, A_1 and A_2, where A_1 and A_2 are the attraction domains of E_0 and E_2, respectively. In contrast, the solution trajectories of stochastic model (1.4), regardless of whether it starts from regions A_2 or A_1, may cross the stable manifold of E_1 finite times, but will always eventually converge to E_0 (see Figure 3).

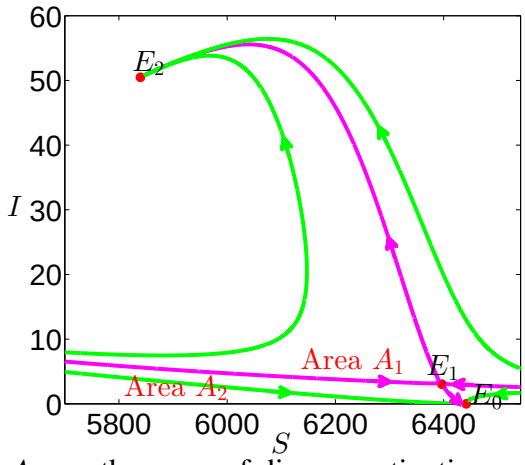

Figure 2. Areas A_1 and A_2 are the areas of disease extinction and persistence, respectively. Stable and unstable manifolds for E_1 of deterministic model (1.3) are represented by the pink curves. Here $\beta = 1.15246 \times 10^{-5}$ and the other parameters are taken from Table 1.

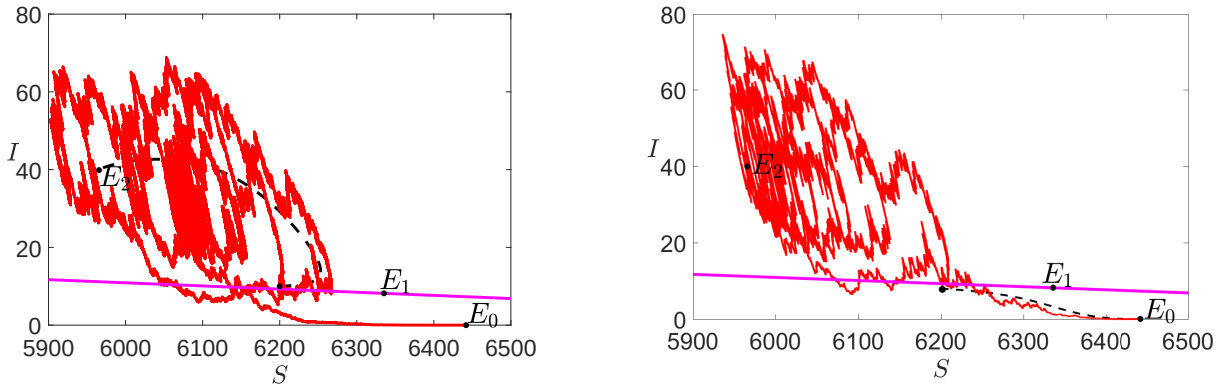

(a) $(S(0), I(0)) = (6200, 10)$ (b) $(S(0), I(0)) = (6200, 8)$

Figure 3. Phase portraits of models (1.3) and (1.4) for different initial values. The pink curve represents stable manifold for E_1. We choose $\beta(\upsilon(t)) \equiv 1.15246 \times 10^{-5}$ and $\sigma = 0.000001$. The remaining parameters are provided in Table 1.

3.2. Impact of random switching on the dynamics of the transmission dynamics for the disease

Next, we consider the effect of the generator $\mathcal{W}$ with the same stationary distribution but different elements on the dynamics of disease transmission. We choose 4 different generators $\mathcal{W}$,

$$G_1 := \begin{pmatrix} -0.292 & 0.292 \\ 0.073 & -0.073 \end{pmatrix}, \; G_2 := \begin{pmatrix} -2.92 & 2.92 \\ 0.73 & -0.73 \end{pmatrix}, G_3 := \begin{pmatrix} -29.2 & 29.2 \\ 7.3 & -7.3 \end{pmatrix}, \; G_4 := \begin{pmatrix} -2920 & 2920 \\ 730 & -730 \end{pmatrix},$$

$\sigma = 0$, $\beta(1) = 1.7623 \times 10^{-5}$, $\beta(2) = 1.0 \times 10^{-5}$, and the other parameters are taken from Table 1. By the irreducible property, we can get that the Markov chain $\upsilon(t)$ always has a unique stationary distribution $(\pi_1, \pi_2) = (0.2, 0.8)$ for these four cases. As shown in Figures 2 and 4, the solutions of stochastic model (1.4) with generators $\mathcal{W}_1$, $\mathcal{W}_2$, $\mathcal{W}_3$, and $\mathcal{W}_4$ may cross the stable manifold of the equilibrium E_1 of deterministic model (1.3) with $\beta = \pi_1\beta(1) + \pi_2\beta(2) = 1.15246 \times 10^{-5}$ finite times. In addition, the stochastic trajectories oscillate in the vicinity of the trajectory of the deterministic model. The amplitude of the oscillations decreases with increasing the elements of the generator $\mathcal{W}$: when the elements are increased to a certain value, the solution of stochastic model (1.4) almost coincides with the solution of deterministic model (1.3) with $\beta = \pi_1\beta(1) + \pi_2\beta(2)$. This implies that when the speed of switching is fast enough, the solution of stochastic model (1.4) with $\sigma = 0$ is practically deterministic.

3.3. Combined effects of white noise and random switching on disease transmission dynamics

Let $\sigma = 0.000001$, $S(0) = 6200$, $I(0) = 10$, and the other parameters are the same as those in Figure 4. In this instance, the basic reproduction number $R_0^s = 0.9186 < 1$. According to Theorem 2.3, we get that the disease is extinct for model (1.4). The numerical simulations shown in Figure 4 directly corroborate the conclusion. In addition, from Figure 2, it is clear that the asymptotic behavior of deterministic model (1.3) with $\beta = \pi_1\beta(1) + \pi_2\beta(2) = 1.15246 \times 10^{-5}$ is closely related to the initial values. In contrast, the disease-free equilibrium E_0 of stochastic model (1.4) with $\beta(1) = \beta(2) = 1.15246 \times 10^{-5}$ is globally asymptotically stable (see Figure 5), that is, the asymptotic behavior of the stochastic model is independent of the initial values. This means that when the deterministic model

shows that both the disease-free equilibrium and the endemic equilibrium are stable, white noise has the power to change the disease-free equilibrium's stability from locally stable to globally stable.

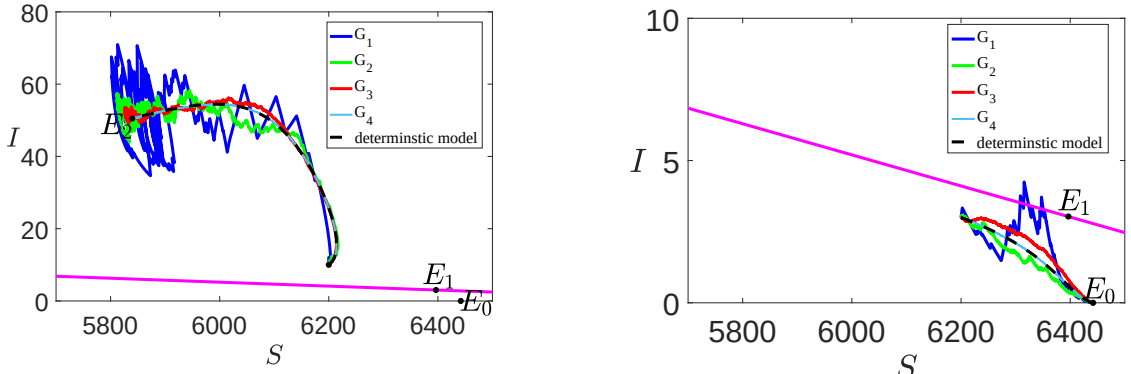

(a): $(S(0), I(0)) = (6200, 10)$ (b): $(S(0), I(0)) = (6200, 3)$

Figure 4. The sample orbits of deterministic model (1.3) and stochastic model (1.4) are graphed for $\mathcal{W} = G_1, G_2, G_3, G_4$. Here $\beta = 1.15246 \times 10^{-5}$, $\beta(1) = 1.7623 \times 10^{-5}$, $\beta(2) = 1.0 \times 10^{-5}$, $\sigma = 0$, and the other parameters are taken from Table 1.

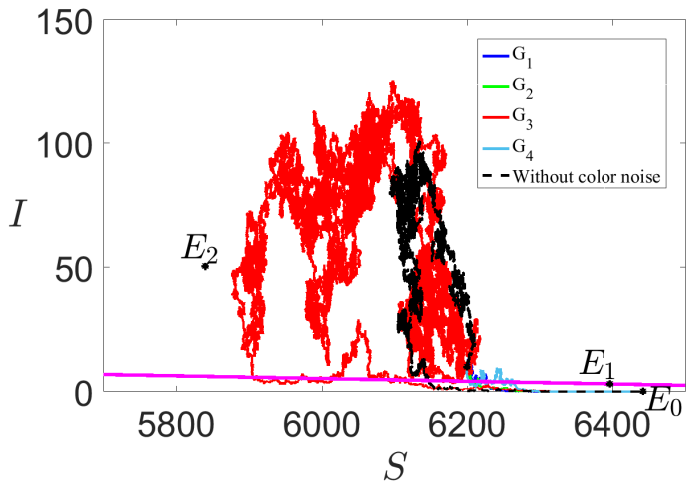

Figure 5. The sample orbits of stochastic model (1.4). Here $\sigma = 0.000001$, $(S(0), I(0)) = (6200, 10)$, and the other parameters are the same as those in Figure 4.

In addition, taking into account the impact of the change of seasons on the survival and transmission rates of SARS-CoV-2, we let $\mathcal{W} = G_5 := \begin{pmatrix} -0.073 & 0.073 \\ 0.292 & -0.292 \end{pmatrix}$, and the other parameters are the same as those in Figure 5. Then, it is easy to get that the Markov chain $\upsilon(t)$ has a unique stationary distribution $(\pi_1, \pi_2) = (0.8, 0.2)$ and $R_0^s = 1.283 > 1$. According to Theorem 2.5, we get that the disease is persistent for model (1.4). The numerical simulation in Figure 6 directly confirms this conclusion. A comparison of Figures 5 and 6 shows that the resurgence of COVID-19 may be caused by random switching of the environment.

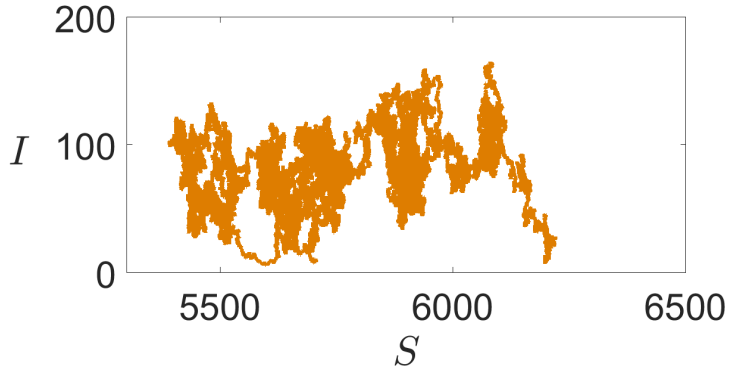

Figure 6. The sample orbits of stochastic model (1.4). Here $\mathcal{W} = \mathcal{W}_5$ and the other parameters are the same as those in Figure 5.

4. Discussion and conclusions

In this article, we investigated the effects of healthcare resources and random environment on the dynamics of the SIR model with logistic growth. Our results showed that the asymptotic behavior of deterministic model (1.3) was closely related to the initial values, since when $R_0 < 1$, deterministic model (1.3) may exhibit bistability; whereas the asymptotic behavior of the stochastic model (1.4) was independent of the initial values, but related to the basic reproduction number R_0^s when $\sigma > 0$.

More specifically, if $r > u_1$, we have

- If $R_0^s > 1$, the disease is persistent; whereas if $R_0^s < 1$, the disease is extinct.
- White noise has the power to alter the disease-free equilibrium's stability.
- If $\sigma = 0$, and the elements of the generator $\mathcal{W}$ are increased to a certain value, then the solution of stochastic model (1.4) almost coincides with the solution of deterministic model (1.3) with $\beta = \sum_{i\in\mathcal{H}} \pi_i \beta(i)$.
- The resurgence of infectious diseases may be caused by random switching of the environment.
- It is vital to maintain adequate medical resources to control the spread of disease, since the lack of medical resources will lead to infectious diseases with complex dynamics, which poses a great challenge to the prevention and control of infectious diseases.

We have also noticed the work of Nguyen et al. [37], where the authors studied a general stochastic differential equation with switching and non-degenerate diffusion. It is shown that the long-term properties of the system can be classified by using a real-valued parameter ξ. However, the techniques used in [37] are not applicable to stochastic model (1.4) since the Lyapunov exponent of $I(t)$ is a non-monotonic function with respect to (S, I) as follows:

$$\lim_{t\to\infty} \frac{\ln I(t)}{t} = \lim_{t\to\infty} \frac{1}{t} \int_0^t \left(\frac{\beta(\upsilon(t))S}{1+\alpha I^2} - (d+\delta) - \left(\mu_0 + \frac{(\mu_1-\mu_0)b}{b+I} \right) - \frac{\sigma^2 S^2}{2(1+\alpha I^2)^2} \right) dt.$$

This paper focused on characterizing disease extinction by studying the stability of the disease-free equilibrium of stochastic model (1.4). In addition, there is no mature theory or methodology for the

study of the ergodicity of stochastic differential equations with switching and degenerate diffusion, and we leave it for future investigations.

Use of AI tools declaration

The authors declare they have not used Artificial Intelligence (AI) tools in the creation of this article.

Acknowledgments

This work is partially supported by the National Natural Science Foundation of China (12071293) and the Natural Science Foundation of Shanghai (23ZR1445100).

Conflict of interest

Sanling Yuan is an editorial board member for Mathematical Biosciences and Engineering and was not involved in the editorial review or the decision to publish this article. All authors declare that there are no competing interests.

References

1. F. Brauer, C. Castillo-Chavez, *Mathematical Models in Population Biology and Epidemiology*, Springer, 2012.
2. R. Acuña-Soto, D. Stahle, M. Cleaveland, M. Therrell, Megadrought and megadeath in 16th century Mexico, *Emerging Infect. Dis.*, **8** (2002), 360. https://doi.org/10.3201/eid0804.010175
3. World Health Organization, *Smallpox Eradication Programme - SEP (1966–1980)*, 2010. Available from: https://www.who.int/news-room/feature-stories/detail/the-smallpox-eradication-programme---sep-(1966-1980).
4. Z. Ma, *Dynamical Modeling and Analysis of Epidemics*, World Scientific, 2009.
5. World Health Organization, *Poliomyelitis*, 2023. Available from: https://www.who.int/news-room/fact-sheets/detail/poliomyelitis.
6. Mayo Clinic, *Diphtheria*, 2023. Available from: https://www.mayoclinic.org/diseases-conditions/diphtheria/symptoms-causes/syc-20351897.
7. World Health Organization, *Measles*, 2023. Available from: https://www.who.int/news-room/fact-sheets/detail/measles.
8. Wikipedia, *Tetanus*, 2024. Available from: https://en.wikipedia.org/wiki/Tetanus.
9. Wikipedia, *HIV/AIDS*, 2024. Available from: https://en.wikipedia.org/wiki/HIV/AIDS.
10. World Health Organization, *Coronavirus Disease (COVID-19) Pandemic*, 2023. Available from: https://www.who.int/emergencies/diseases/novel-coronavirus-2019.
11. R. Anderson, R. May, *Infectious Diseases of Humans: Dynamics and Control*, Oxford University Press, 1991.
12. R. Ross, *The Prevention of Malaria*, John Murray, 1911.

13. W. Kermack, A. McKendrick, A contribution to the mathematical theory of epidemics, *Proc. R. Soc. London, Ser. A*, **115** (1927), 700–721. https://doi.org/10.1098/rspa.1927.0118

14. W. Kermack, A. McKendrick, Contributions to the mathematical theory of epidemics. II. the problem of endemicity, *Proc. R. Soc. London, Ser. A*, **138** (1932), 55–83. https://doi.org/10.1098/rspa.1932.0171

15. R. Anderson, C. Fraser, A. Ghani, C. Donnelly, S. Riley, N. Ferguson, et al., Epidemiology, transmission dynamics and control of SARS the 2002–2003 epidemic, *Philos. Trans. R. Soc. London, Ser. B*, **359** (2004), 1091–1105. https://doi.org/10.1098/rstb.2004.1490

16. M. Aguiar, V. Anam, K. Blyuss, C. Estadilla, B. Guerrero, D. Knopoff, et al., Mathematical models for dengue fever epidemiology: A 10-year systematic review, *Phys. Life Rev.*, **40** (2022), 65–92. https://doi.org/10.1016/j.plrev.2022.02.001

17. J. Dushoff, J. Plotkin, S. Levin, D. Earn, Dynamical resonance can account for seasonality of influenza epidemics, *PNAS*, **101** (2004), 16915–16916. https://doi.org/10.1073/pnas.0407293101

18. M. Gatto, E. Bertuzzo, L. Mari, S. Miccoli, L. Carraro, R. Casagrandi, et al., Spread and dynamics of the COVID-19 epidemic in Italy: Effects of emergency containment measures, *PNAS*, **117** (2020), 10484–10491. https://doi.org/10.1073/pnas.2004978117

19. C. Shan, H. Zhu, Bifurcations and complex dynamics of an SIR model with the impact of the number of hospital beds, *J. Differ. Equations*, **257** (2014), 1662–1688. https://doi.org/10.1016/j.jde.2014.05.030

20. G. Lan, S. Yuan, B. Song, The impact of hospital resources and environmental perturbations to the dynamics of SIRS model, *J. Franklin Inst.*, **358** (2021), 2405–2433. https://doi.org/10.1016/j.jfranklin.2021.01.015

21. W. Wang, S. Ruan, Bifurcations in an epidemic model with constant removal rate of the infectives, *J. Math. Anal. Appl.*, **291** (2004), 775–793. https://doi.org/10.1016/j.jmaa.2003.11.043

22. A. Abdelrazec, J. Bélair, C. Shan, H. Zhu, Modeling the spread and control of dengue with limited public health resources, *Math. Biosci.*, **271** (2016), 136–145. https://doi.org/10.1016/j.mbs.2015.11.004

23. Z. Shi, D. Jiang, Stochastic modeling of SIS epidemics with logarithmic ornstein–uhlenbeck process and generalized nonlinear incidence, *Math. Biosci.*, **365** (2023), 109083. https://doi.org/10.1016/j.mbs.2023.109083

24. Q. Liu, D. Jiang, Threshold behavior in a stochastic SIR epidemic model with logistic birth, *Physica A*, **540** (2020), 123488. https://doi.org/10.1016/j.physa.2019.123488

25. S. Liu, S. Ruan, X. Zhang, Nonlinear dynamics of avian influenza epidemic models, *Math. Biosci.*, **283** (2017), 118–135. https://doi.org/10.1016/j.mbs.2016.11.014

26. P. Saha, U. Ghosh, Global dynamics and control strategies of an epidemic model having logistic growth, non-monotone incidence with the impact of limited hospital beds, *Nonlinear Dyn.*, **105** (2021), 971–996. https://doi.org/10.1007/s11071-021-06607-9

27. L. Gao, H. Hethcote, Disease transmission models with density-dependent demographics, *J. Math. Biol.*, **30** (1992), 717–731. https://doi.org/10.1007/bf00173265

28. J. Cao, X. Jiang, B. Zhao, Mathematical modeling and epidemic prediction of COVID-19 and its significance to epidemic prevention and control measures, *J. Biomed. Res. Innovation*, **1** (2020), 1–19. https://doi.org/10.31579/2690-1897/021
29. M. Zanin, C. Xiao, T. Liang, S. Ling, F. Zhao, Z. Huang, et al., The public health response to the COVID-19 outbreak in mainland China: A narrative review, *J. Thoracic Dis.*, **12** (2020), 4434. https://doi.org/10.3201/eid0804.010175
30. S. Welliver, C. Robert, Temperature, humidity, and ultraviolet B radiation predict community respiratory syncytial virus activity, *Pediatr. Infect. Dis. J.*, **26** (2007), S29–S35. https://doi.org/10.1097/inf.0b013e318157da59
31. L. Nottmeyer, F. Sera, Influence of temperature, and of relative and absolute humidity on COVID-19 incidence in England—A multi-city time-series study, *Environ. Res.*, **196** (2021), 110977. https://doi.org/10.1016/j.envres.2021.110977
32. J. Han, J. Yin, X. Wu, D. Wang, C. Li, Environment and COVID-19 incidence: A critical review, *J. Environ. Sci.*, **124** (2023), 933–951. https://doi.org/10.1016/j.jes.2022.02.016
33. G. Lan, S. Yuan, B. Song, Threshold behavior and exponential ergodicity of an sir epidemic model: the impact of random jamming and hospital capacity, *J. Math. Biol.*, **88** (2024), 2. https://doi.org/10.1007/s00285-023-02024-1
34. N. Dieu, D. Nguyen, N. Du, G. Yin, Classification of asymptotic behavior in a stochastic SIR model, *SIAM J. Appl. Dyn. Syst.*, **15** (2016), 1062–1084. https://doi.org/10.1137/15m1043315
35. W. Wei, W. Xu, J. Liu, A regime-switching stochastic SIR epidemic model with a saturated incidence and limited medical resources, *Int. J. Biomath.*, **16** (2023), 2250124. https://doi.org/10.1142/S1793524522501248
36. T. Tuong, D. Nguyen, N. Dieu, K. Tran, Extinction and permanence in a stochastic SIRS model in regime-switching with general incidence rate, *Nonlinear Anal. Hybrid Syst.*, **34** (2019), 121–130. https://doi.org/10.1016/j.nahs.2019.05.008
37. D. Nguyen, N. Nguyen, G. Yin, General nonlinear stochastic systems motivated by chemostat models: Complete characterization of long-time behavior, optimal controls, and applications to wastewater treatment, *Stochastic Processes Appl.*, **130** (2020), 4608–4642. https://doi.org/10.1016/j.spa.2020.01.010
38. G. Yin, C. Zhu, *Hybrid Switching Diffusions: Properties and Applications*, Springer Science & Business Media, 2009.
39. S. Bonaccorsi, S. Ottaviano, A stochastic differential equation SIS model on network under markovian switching, *Stochastic Anal. Appl.*, **41** (2023), 1231–1259. https://doi.org/10.1080/07362994.2022.2146590
40. A. Gray, D. Greenhalgh, L. Hu, X. Mao, J. Pan, A stochastic differential equation SIS epidemic model, *SIAM J. Appl. Math.*, **71** (2011), 876–902. https://doi.org/10.1137/10081856x
41. Wikipedia, *COVID-19 Pandemic in Tamil Nadu*, 2023. Available from: https://en.wikipedia.org/wiki/COVID-19_pandemic_in_Tamil_Nadu.
42. Knoema, *Tamil Nadu–Crude Birth Rate*, 2024. Available from: https://knoema.com/atlas/India/Tamil-Nadu/Birth-rate.

43. Knoema, *Tamil Nadu–Crude Death Rate*, 2024. Available from: http://knoema.com/atlas/India/Tamil-Nadu/Death-rate.

44. N. George, N. Tyagi, J. Prasad, COVID-19 pandemic and its average recovery time in Indian states, *Clin. Epidemiol. Global Health*, **11** (2021), 100740. https://doi.org/10.1016/j.cegh.2021.100740

45. M. Barman, T. Rahman, K. Bora, C. Borgohain, COVID-19 pandemic and its recovery time of patients in India: A pilot study, *Diabetes Metab. Syndrome: Clin. Res. Rev.*, **14** (2020), 1205–1211. https://doi.org/10.1016/j.dsx.2020.07.004

46. S. Marimuthu, M. Joy, B. Malavika, A. Nadaraj, E. Asirvatham, L. Jeyaseelan, Modelling of reproduction number for COVID-19 in India and high incidence states, *Clin. Epidemiol. Global Health*, **9** (2021), 57–61. https://doi.org/10.1016/j.cegh.2020.07.004

47. A. Chin, J. Chu, M. Perera, K. Hui, H. Yen, M. Chan, et al., Stability of SARS-Cov-2 in different environmental conditions, *Lancet Microbe*, **1** (2020), e10. https://doi.org/10.1016/s2666-5247(20)30003-3

48. S. Riddell, S. Goldie, A. Hill, D. Eagles, T. Drew, The effect of temperature on persistence of SARS-Cov-2 on common surfaces, *Virol. J.*, **17** (2020), 1–7. https://doi.org/10.1186/s12985-020-01418-7

AIMS Press